Supporting Information

Overcoming synthetic metastabilities and revealing metal-to-insulator transition & thermistor bi-functionalities for *d*-band correlation perovskite nickelates

Jikun Chen[1†], Haiyang Hu[1†], Jiaou Wang[2], Takeaki Yajima[3], Binghui Ge[4], Xinyou Ke[5], Hongliang Dong[6], Yong Jiang[1]*, and Nuofu Chen[7]**

[1]School of Materials Science and Engineering, University of Science and Technology Beijing, Beijing 100083, China
[2]Beijing Synchrotron Radiation Facility, Institute of High Energy Physics, Chinese Academy of Sciences, Beijing 100049, China
[3]School of Engineering, The University of Tokyo, 2-11-16 Yayoi, Bunkyo-ku, Tokyo 113-0032, Japan
[4]Beijing National Laboratory for Condensed Matter Physics, Chinese Academy of Sciences, Beijing 100190, China
[5]Department of Mechanical and Aerospace Engineering, Case Western Reserve University, Cleveland, Ohio 44106, United States
[6]Center for High Pressure Science and Technology Advanced Research, Shanghai 201203, China
[7]School of Renewable Energy, North China Electric Power University, Beijing 102206, China

Correspondence: Prof. Jikun Chen (jikunchen@ustb.edu.cn), Prof. Yong Jiang (yjiang@ustb.edu.cn), and Prof. Nuofu Chen (nfchen@ncepu.edu.cn).
†J. Chen and H. Hu contribute equally to this work.

Section A: Experimental details

The involved compositions for the presently grown *Re*NiO_3 thin films include $NdNiO_3$, $SmNiO_3$, $EuNiO_3$, $GdNiO_3$, $Sm_{0.75}Nd_{0.25}NiO_3$, $Sm_{0.5}Nd_{0.5}NiO_3$, $Sm_{0.25}Nd_{0.75}NiO_3$, $Sm_{0.75}Eu_{0.25}NiO_3$, $Sm_{0.5}Nd_{0.25}Eu_{0.25}NiO_3$ and $Sm_{0.5}Nd_{0.25}Gd_{0.25}NiO_3$. The *Re*$NiO_3$ thin films were grown by using the following steps. Firstly, the precursors of *Re*$(NO_3)_3$ and $Ni(CH_3COO)_2$, with purity > 99.9%, were mixed at the nominal stoichiometry of 1:1, and resolved within ethylene glycol monomethyl ether (EGME) at a concentration of 0.2 M/L under ultrasonic. As obtained solutions were spin coated onto perovskite structured single crystalline substrates, such as $LaAlO_3$ (LAO), $SrTiO_3$ (STO) and $(LaAlO_3)_{0.3}(Sr_2AlTaO_6)_{0.7}$ (LSAT), at an orientation of (001). The thicknesses of all the substrates were 0.5 mm, while their surfaces were polished without additional chemical treatment. The rotation speed for the spin coating process was about 4000 r/minute, and the spin coated samples were further baked at a temperature of 175 °C to evaporate the solvent of EGME. Finally, the samples were annealed at 800 °C and an oxygen pressure of 15 MPa for 3 hours, the process of which crystallized the film into perovskite *Re*NiO_3. This condition guarantees the crystallization of all the involved *Re*NiO_3 as demonstrated in the present work, while *Re*NiO_3 with larger rare-earth radius can be synthesized at a smaller pressure.

The cross-plane structures of as-grown films were characterized by using X-ray diffraction (XRD), while the information associated to the in-plan direction was characterized by using reciprocal space mapping (RSM). In the RSM analysis, the [114] reciprocal space vectors of the film and substrate were projected at [110] and [001], for the in-plane and cross-plane direction, respectively. The cross-plane morphology of as-grown $Re\text{NiO}_3$/LAO was observed by using techniques of high-angle annular dark-field (HAADF) and annular bright-field (ABF) scanning transmission electron microscopy (STEM) performed on JEM-ARM 200F TEM operated at 200 kV with a cold field emission gun and aberration correctors for both probe-forming and imaging lenses. The near edge X-ray absorption fine structure (NEXAFS) was performed at Beijing Synchrotron Radiation Facility, Institute of High Energy Physics, Chinese Academy of Sciences, Beijing 100049, China. The resistance of as-grown thin films was measured by using a commercialized CTA-system within the temperature range from 300 K- 550 K in vacuum. A four point approach was used to measure the resistance by applying five currents (I) at the both ends and reading out the respective voltage (V) from the two middle electrodes. The magnitude of the resistance was obtained from the slope of the V-I linear relation. Before measuring each point, the applied magnitude of current is automatically adjusted by the system based on the resistance for reaching the optimum range, and the uncertainty of measurement is below 5%. To vary the temperature, a heating (or cooling) speed of 2 °C/minute was used, while the temperature was stabilized for an additional 1 minute before starting the measurement of the resistance for each settled temperature step. This configuration ensures that the resistance was acquired at a stabilized temperature within a relative short time of 10 second. To characterize the resistance of as-grown thin films from the temperature range within 5 K – 400 K in vacuum by using a PPMS system (Quantum Design).

Section B: Additional results

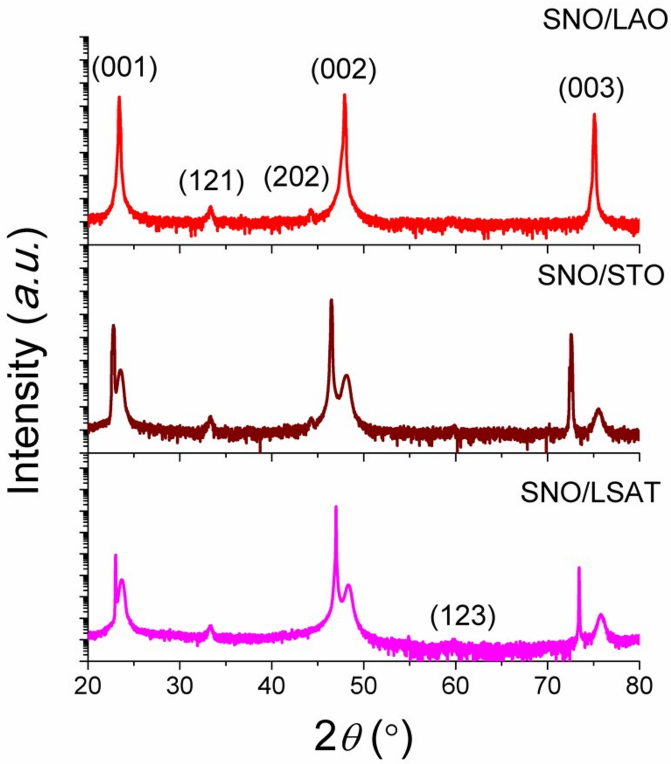

Figure S1. X-ray diffraction patterns of as-grown $SmNiO_3$ (SNO) on $LaAlO_3$ (001), $SrTiO_3$ (001) and $(LaAlO_3)_{0.3}(Sr_2AlTaO_6)_{0.7}$ (001). The indexation is referred to Acad. Sci. Ser. C, 1971, 272, 2163. IDespite the low intensities also observed for the (121) and (202) planes, the diffraction peak associated to the (001) plane of the thin films mainly appears besides ones for the substrate.

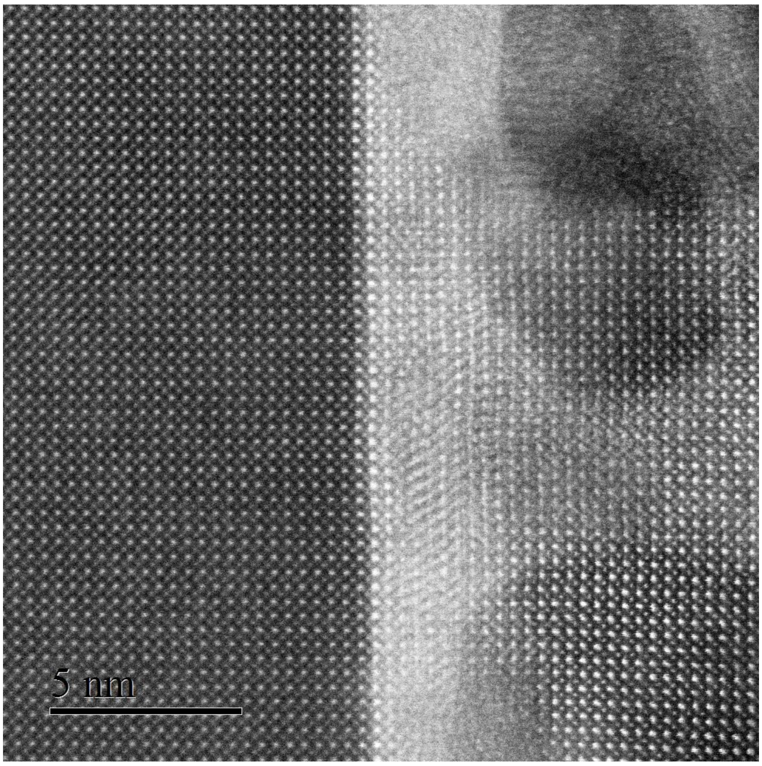

Figure S2. The high-angle annular dark-field (HAADF) images of the interfacial regions of $SmNiO_3/SrTiO_3$ (001);

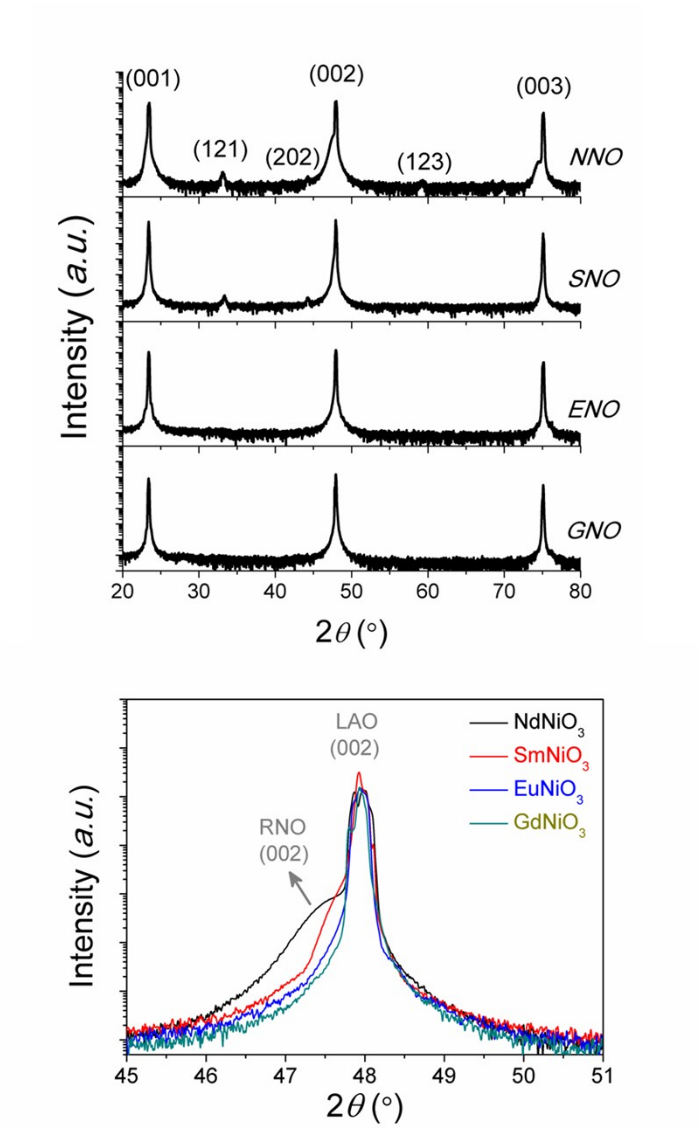

Figure S3. X-ray diffraction patterns of as-grown *Re*NiO_3 (*Re*=Nd, Sm, Eu and Gd) on $LaAlO_3$ (001). Reducing the atomic radius of the rare-earth element shifts the diffraction peak associated to the thin film to the right, indicating a respective reduction in their lattice constant.

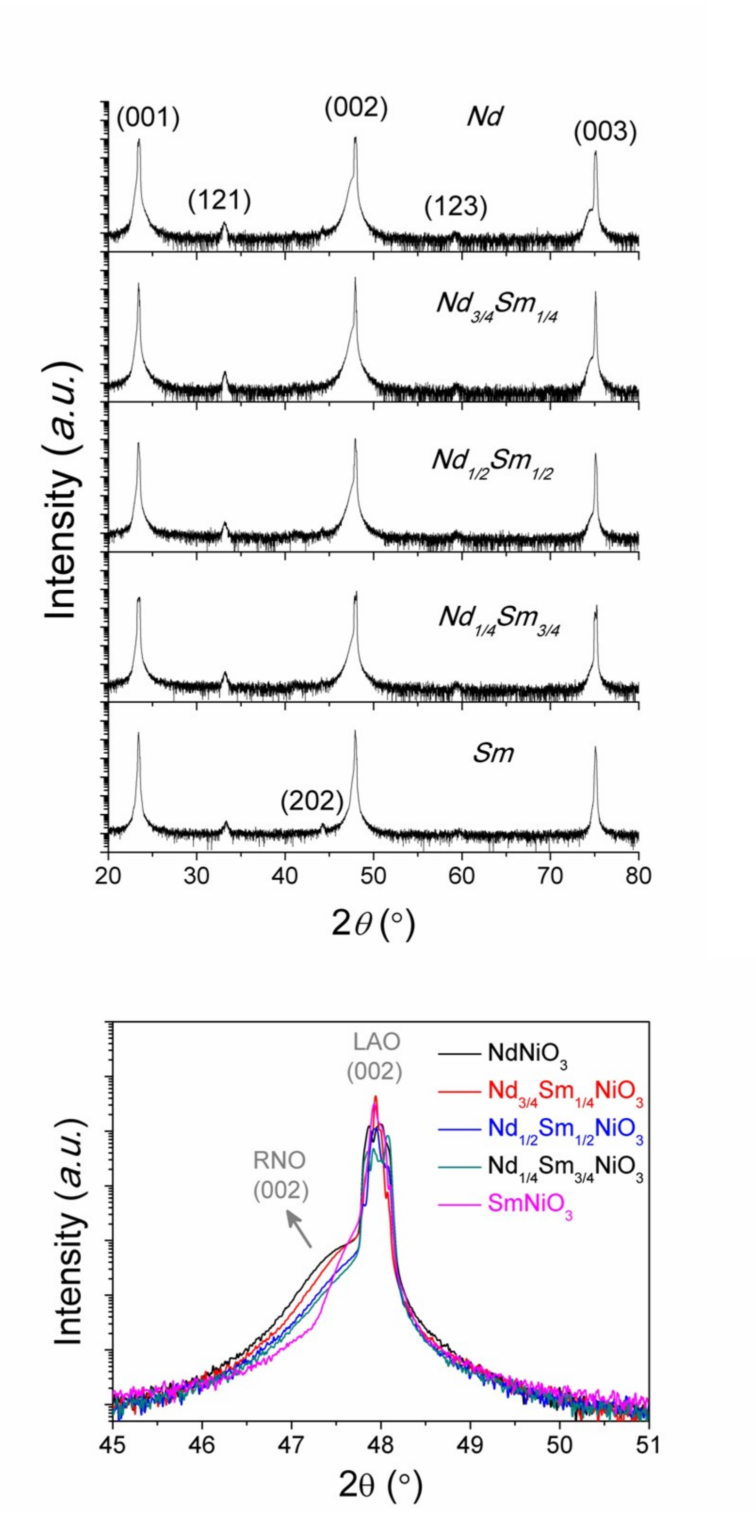

Figure S4. X-ray diffraction patterns of as-grown $Nd_xSm_{1-x}NiO_3$ (x=0, 1/4, 1/2, 3/4 and 1) on $LaAlO_3$ (001). Enhancing the composition of Sm as compared to Nd shifts the diffraction peak associated to the thin film to the right, indicating a respective reduction in their lattice constant.

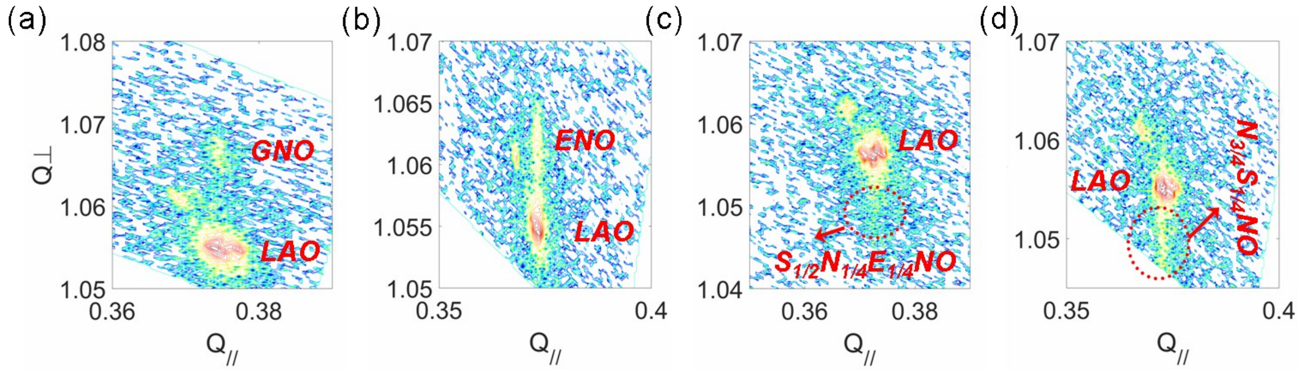

Figure S5. Representative examples of the reciprocal space mapping (RSM) for several *Re*NiO_3/LAO samples: **(a)** $GdNiO_3$/LAO, **(b)** $EuNiO_3$/LAO, **(c)** $Sm_{0.5}Nd_{0.25}Eu_{0.25}NiO_3$/LAO, **(d)** $Nd_{0.75}Sm_{0.25}NiO_3$/LAO.

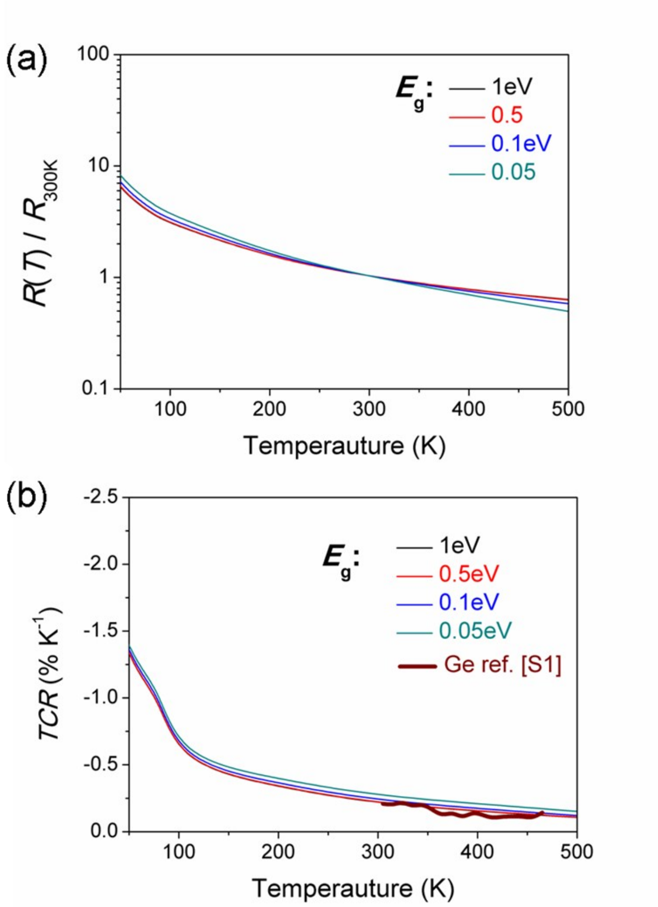

Figure S6. (a) The *R*-*T* tendency and (b) the TCR-*T* tendency estimated for conventional semiconductors with various band gaps by considering only the thermal activation of electrons from the valance band to the conduction band.

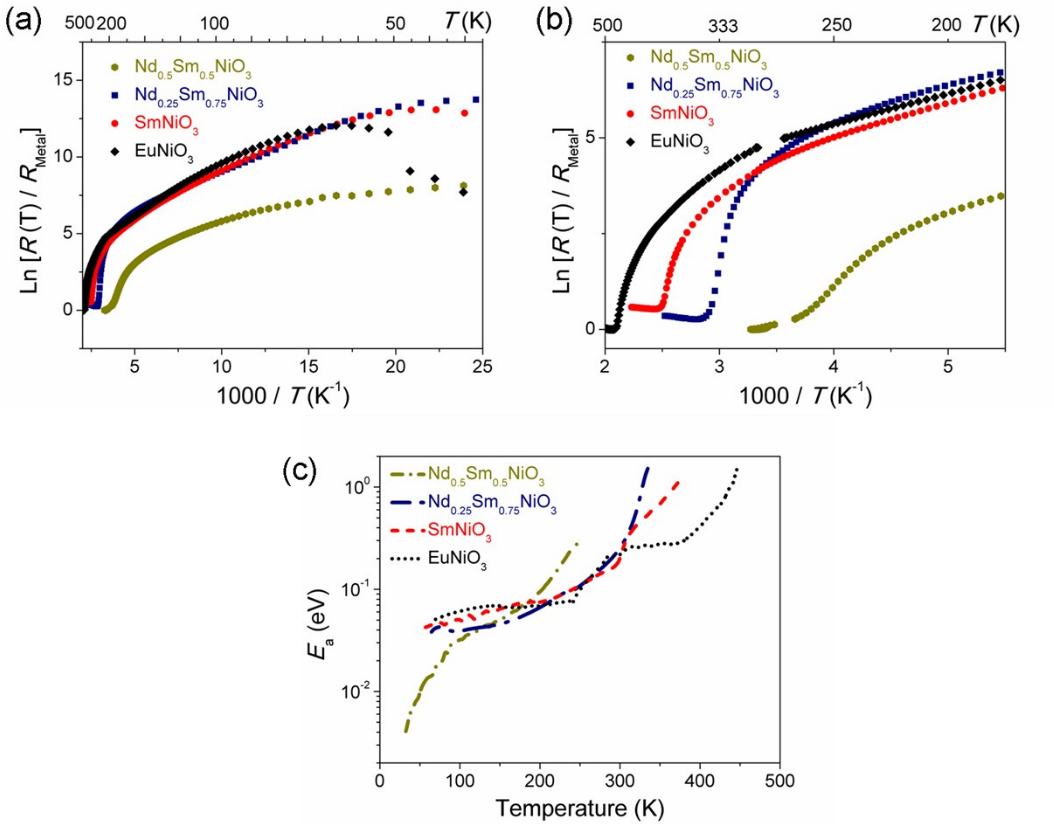

Figure S7. (a),(b) $Ln[R(T)/R_{\mathrm{metal.}}]$ – $1000/T$ relationships for the samples shown in Figure 5b; **(c)** carrier activation energy (E_a) calculated via $E_a=d(\ln R)/d(1/T)$. It can be seen that the magnitude of E_a is temperature dependent, and varies from 10^{-2} to 10^{-1} eV within the temperature range from 80-200 K.

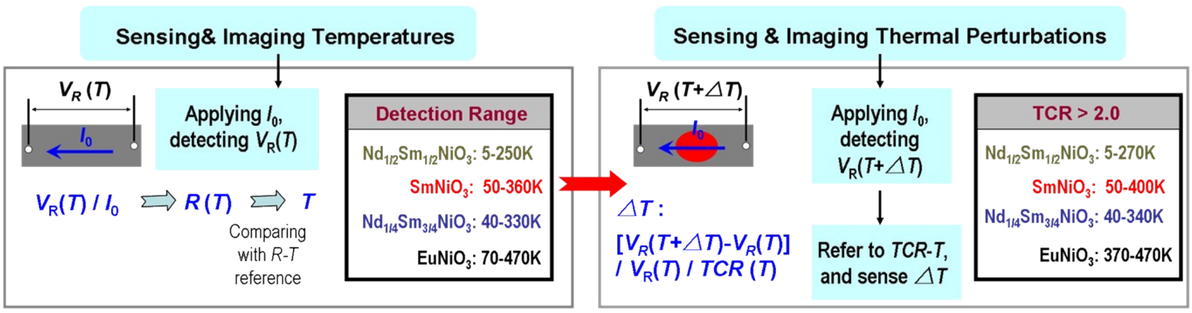

Figure S8. One example illustrated for detection of thermal perturbations based on the present grown *Re*NiO_3. The temperature can be obtained by measuring the resistivity of *Re*NiO_3 and referring to its respective *R-T* relationship. In addition, its large magnitude of TCR at a specific temperature can be also utilized to sense the localized thermal perturbations, i.e. caused by IR irradiations.

Reference

[S1] K. Toko, I. Nakao, T. Sadoh, T. Noguchi, M. Miyao, Electrical properties of poly-Ge on glass substrate grown by two-step solid-phase crystallization. *Solid State Electronics*, 2009, **53**, 1159–1164